Resistive plate chambers for time-of-flight measurements

A. Blanco[a], P. Fonte[a,b,*], L. Lopes[a,c], A. Mangiarotti[d],
R. Ferreira-Marques[a,c], A. Policarpo[a,c]

[a] *LIP—Laboratório de Instrumentação e Física Experimental de Partículas, Dep. de Fisica, Universidade de Coimbra,
Coimbra P-3004-516, Portugal*
[b] *Instituto Superior de Engenharia de Coimbra, Coimbra, Portugal*
[c] *CFRM, Departamento de Física da Universidade de Coimbra, Coimbra, Portugal*
[d] *Dipartimento di Fisica, Università degli Studi di Firenze, Largo E.Fermi 2, 50125 Firenze, Italy*

Abstract

The applications of Resistive Plate Chambers (RPCs) have recently been extended by the development of counters with time resolution below 100 ps σ for minimum ionising particles. Applications to HEP experiments have already taken place and many further applications are under study. In this work, we address the operating principles of such counters along with some present challenges, with emphasis on counter ageing. Possible applications to radioisotope imaging will be outlined.
© 2003 Elsevier B.V. All rights reserved.

PACS: 29.40.Cs

Keywords: RPC; TOF; PET; Ageing

1. Introduction

Resistive Plate Chambers (RPCs) with time resolution below 100 ps σ for minimum ionising particles have been recently developed [1,2]. This type of detector, operating at atmospheric pressure with non-flammable gases, seems well suited for high-granularity time-of-flight (TOF) systems, providing performances comparable to the scintillator-based TOF technology but offering a significantly lower price per channel, compact mechanics and magnetic field compatibility. A recent review may be found in Ref. [3].

Time resolutions of 300 ps FWHM have been also demonstrated for 511 keV photon pairs, with possible application to whole-body human PET imaging. The sub-millimetric imaging of small animals may be also an attractive possibility [4].

2. Some considerations on the working principles

2.1. Efficiency

It has been recognised long ago that the large efficiency values reached by RPCs for minimum ionising particles (MIPs) cannot be explained

*Corresponding author. LIP-Coimbra, Dep. de Fisica, Universidade de Coimbra, Coimbra P-3004-516, Portugal. Tel.: +351-239-833-465; fax: +351-239-829-158.

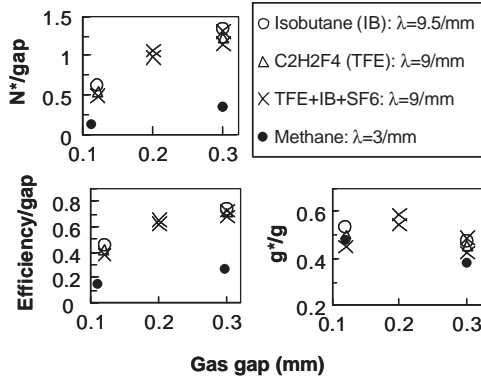*E-mail address:* fonte@lipc.fis.uc.pt (P. Fonte).

Fig. 1. Efficiency data taken from Ref. [3] for different gases and gap widths (g) along with the corresponding sensitive fraction of the gas gap (g^*/g) and the average effective number of primary clusters (N^*) per gap. Data for λ was taken from Ref. [8] (highly relativistic particles).

without resorting to some form of avalanche growth saturation, possibly due to the space charge effect [5], which extends the sensitive region (close to the cathode).

The width of the sensitive region may be estimated by requiring that the measured inefficiency $(1 - \varepsilon)$ equals the probability that a passing particle deposits no ionisation in it. The required average number of "effective" ionisation clusters is then

$$N^* = -\ln(1 - \varepsilon) \tag{1}$$

and the width of the sensitive region $g^* = N^*/\lambda$, where λ is the cluster density per unit length.

Fig. 1 shows some data on timing RPC efficiency for different gases and gap widths from which N^* and the sensitive fraction of the gas gap, g^*/g, may be calculated. In all cases the sensitive region corresponds to about half of the gap width.

2.2. Timing resolution

A simple theory of the RPC timing properties may be formulated on the following principles (see also Refs. [6–8]).

1. The Poissonian probability that $k > 0$ clusters will be produced in the sensitive region of the gap from the N^* average effective clusters is given by

$$P(k) = \frac{(N^*)^k}{(\exp(N^*) - 1)\, k!}. \tag{2}$$

2. Avalanches initiated by (in first approximation) single electrons will result in an exponentially distributed final avalanche charge (Furry law [9]) after a fixed development length.[1] Since the gain fluctuations occur mainly in the first few amplification steps (see Ref. [8] for a detailed study) the effective initial number of electrons, k, may be replaced by an apparent value, n, that takes into account both the cluster and the avalanche statistics,

$$n = \sum_{1}^{k} h \tag{3}$$

where h is an exponentially distributed random variable with unit mean value. The distribution of n may be calculated analytically [10], yielding

$$P(n) = e^{-n} \frac{N^* I_1(2\sqrt{nN^*})}{(\exp(N^*) - 1)\sqrt{nN^*}} \tag{4}$$

where I_1 is the modified Bessel function of the first kind. In the limit of very small N^* the probability of releasing more than one cluster vanishes and $P(n) \to e^{-n}$, recovering the Furry law.

3. The n apparent initial charges are deterministically multiplied in time by a factor $\exp(\alpha^* v t)$, where α^* is the effective multiplication coefficient (first Townsend coefficient minus the electrons attachment coefficient), v the electron drift velocity and t the elapsed time. The induced current is therefore given by $i(t) = n i_e \exp(\alpha^* v t)$, with i_e being the current induced by a single drifting electron.

4. Owing to the exponential growth of current in time the comparator will sense also an exponentially growing voltage with the same value of $\alpha^* v$ [11]. Therefore, the threshold voltage maybe related to an equivalent threshold current i_{th} at the amplifier input.

---

[1] Calculations suggest that the detailed form of the avalanche gain statistics has a negligible influence on the time resolution ([6,8]), being reasonable to consider the simplest case.

5. It is assumed that the space charge effect will become important only for induced currents larger than i_{th}.

6. When the threshold current is reached, a time T is registered in accordance with

$$i_{th} = n i_e \exp(\alpha^* v T) = n i_e \exp(\tau) \tag{5}$$

where the reduced variable τ was introduced, corresponding to the measured time in units of $1/(\alpha^* v)$.

Eq. (5) relates functionally the reduced measured time τ to the distribution Eq. (4) and therefore the distribution of τ may be calculated by a change of variable. Restating Eq. (5) as $\exp(\tau') = n \exp(\tau)$ one finds

$$P(\tau) = e^{(\tau'-\tau)-\exp(\tau'-\tau)} \frac{N^* I_1(2\sqrt{N^* e^{(\tau'-\tau)}})}{(\exp(N^*)-1)\sqrt{N^* e^{(\tau'-\tau)}}}. \tag{6}$$

In the single cluster limit ($N^* \to 0$):

$$P(\tau) \to e^{(\tau'-\tau)-\exp(\tau'-\tau)} \tag{7}$$

reproducing the result derived in Ref. [6].

A graphical representation of Eq. (6) is shown in Fig. 2, along with an equivalent Monte-Carlo calculation adapted from Ref. [12]. However, the Monte-Carlo is more accurate in that all clusters are followed to the anode and N^* is determined from the simulation output. The good agreement shows that the "effective number of primary clusters" approach is highly accurate.

Since any change on the threshold level affects only τ' it is clear from the functional form of Eq. (6) that this results merely on a shift of the time distribution. Therefore any moment about

the mean will depend only on N^* (or, equivalently, on the counter inefficiency) and can be written, going back to the measured time T:

$$E[(T - E(T))^m] = \frac{K_m(N^*)}{\alpha^* v} = \frac{K_m(-\ln(1-\varepsilon))}{\alpha^* v}. \tag{8}$$

The reduced standard deviation $K_2(N^*)$ may be calculated as a series [7], being the results shown in Fig. 3 along with a Gaussian fit to $P(\tau)$ (Eq. (6)).

Presented in Fig. 4 is a comparison between experimental data and the present model. The average value of $\alpha^* v$ was determined using the method described in [11] along with the time resolution data, using the set-up described in
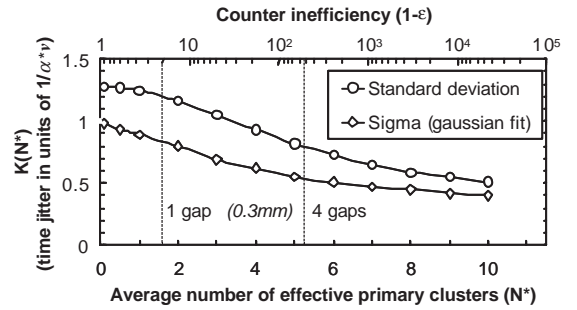
Fig. 3. Width of $P(\tau)$ (Eq. (6)) evaluated by its standard deviation $K_2(N^*)$ (Eq. (8)), following [7], and by fitting a gaussian curve (the method used to analyse experimental data). The expected values for N^* (from Fig. 1) are marked for 1 and 4 (0.3 mm) gap counters.

Fig. 4. Comparison, based on Eq. (8), between the measured average values of $\alpha^* v$ (lines) and the counter time resolution (with and without charge correction). A reasonable value of $K(N^*) = 0.75$ reproduces well the uncorrected data (compare with Fig. 3).
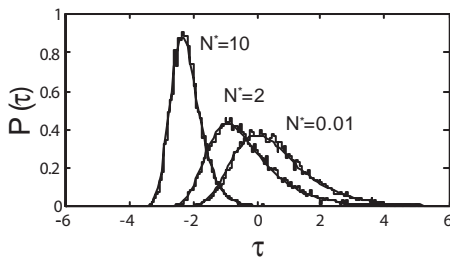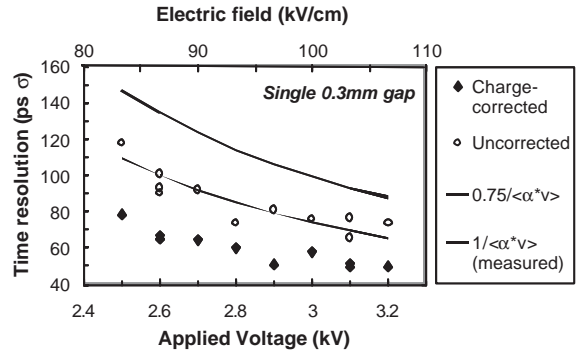

Fig. 2. Distribution, from Eq. (6), of the reduced measured time $\tau = \alpha^* v T$ (thick line), for different values of N^*. The superimposed histograms correspond to an equivalent Monte-Carlo calculation.

Ref. [13]. The theory reasonably describes the data when no charge correction is applied to the measured time. This is natural, since the time–charge correlation was not considered in the model.

The present treatment expands upon previous work [7] in that an explicit expression for $P(\tau)$ is obtained. This allows the measurement of the distribution width by a Gaussian adjustment, providing a more accurate comparison with the experimentally available data.

3. Present challenges

A number of challenges still stand on the way of full-scale applications of high resolution TOF with RPCs. Some of the most important ones include:

- the demonstration that a high-granularity RPC-TOF counter is able to operate without loss of time resolution in a high occupancy environment despite potentially large crosstalk levels;
- investigation of possible ageing effects (see below).

For many applications it would be also of fundamental importance the extension of the counting rate capabilities from around $200\,Hz/cm^2$ (for most glass-made counters) to much larger values and the development of effective methods for controlling the timing tails (see Ref. [13] for a possible approach).

3.1. Ageing studies

Severe ageing of glass RPCs operating in streamer mode has been observed and related to the presence of water vapour traces in the gas mixture. An unidentified deposit was found over the glass surface, severely increasing the dark count rates and reducing the counter efficiency [14].

Naturally it is of great practical importance the investigation of such effect in timing RPCs, often made with glass electrodes and working in somewhat similar gaseous mixtures. To this aim we built a test set-up comprising six single-gap counters, each made with one glass and one aluminium electrode. Three counters were con-

nected with the glass electrode as a cathode and three were connected with the glass electrode as an anode.

All counters were illuminated laterally, along the gas gap, by a mercury UV lamp that created primary charges by photoelectric effect at the cathodes. The different cathode photosensitivities were compensated by slightly adjusting the applied voltages, ranging from 2.8 to 3.0 kV, until all chambers registered similar current values. For the settings chosen the currents were essentially independent from any small variations in the lamp intensity, having reached the maximum value allowed by the resistive electrode.

The counters were illuminated for 22 h and kept in darkness 2 h per day, being continuously recorded the counter currents, temperature, atmospheric pressure and lamp intensity. The set-up was kept in a continuous flow of "standard" timing RPC gas, $C_2H_2F_4 + 10\%SF_6 + 5\%iso-C_4H_{10}$, being added enough water vapour to keep a 10% relative humidity. The gas container was made of acrylic plastic with Viton o-ring seals and several common types of glues, plastics and metals were used internally as needed.

The dark current values recorded daily at the end of the 2-h dark period were corrected for systematic variations due to temperature, being the results for six months of operation shown in Fig. 5. There is no evidence of any systematic
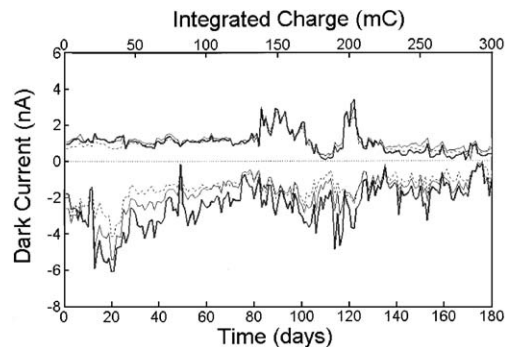
Fig. 5. Dark current as a function of time and accumulated charge for 6 counters (positive: glass cathode, negative: aluminium cathode). No systematic increase in dark current is visible, contrasting with the ageing effect observed in streamer-mode RPCs [14]. The integrated charge corresponds to 1700 days of operation at the typical counter operational settings.

long-term increase of dark current, suggesting that the ageing effect mentioned above is less severe in timing RPCs than in streamer-mode RPCs. The short-term dark current fluctuations are well correlated for the three chambers of the same type (glass or aluminium cathode) and therefore should be of environmental origin.

However, a visual inspection of the electrodes confirmed the existence of a whitish, dry, deposit over the glass cathodes. The deposit covered an area of approximately $1\,cm^2$ close to the UV-light entrance slit, presumably corresponding to the effectively illuminated region. The glass anodes were also thinly covered with a viscous-looking substance everywhere excepted in the $1\,cm^2$ irradiated region. The aluminium electrodes seemed perfectly clear.

The average integrated charge of $140\,mC$ (changes slightly from chamber to chamber) corresponds to 1700 days of operation at $200\,Hz/cm^2$ and 10 pC/avalanche.

4. Conclusions

Experimental efficiency data shows that timing RPCs are sensitive to primary ionisation clusters created in about half of the gas gap (cathode-side). For 0.3 mm-gap devices filled with common gases the average number of primary clusters created in this region (N^*) is close to 1/gap for MIPs.

A simple, analytically solvable, model of the time resolution suggests that it should depend only on some function $K(N^*)$ divided by $\alpha^* v$. Multiple gaps are taken in consideration simply through the value of N^*. The model reproduces well the available experimental data when the charge-time correlation is not considered.

Ageing studies were performed on six counters made with glass and aluminium electrodes. After a charge transfer equivalent to 800 days of normal operation no increase of dark current was detected. However, an unidentified deposit was found over the glass cathodes, being absent on the irradiated regions of the glass anodes and on all aluminium electrodes.

References

[1] P. Fonte, A. Smirnitski, M.C.S. Williams, Nucl. Instr. and Meth. A 443 (2000) 201.
[2] P. Fonte, et al., Nucl. Instr. and Meth. A 449 (2000) 295.
[3] P. Fonte, Applications and new developments in resistive plate chambers, IEEE Trans. Nucl. Sci. NS-49 (3) (2002) 881.
[4] A. Blanco, et al., Nucl. Instr. and Meth. A 508 (2003) 88.
[5] M. Abbrescia, et al., Nucl. Phys. B (Proc. Suppl.) 78 (1999) 459.
[6] A. Mangiarotti, A. Gobbi, Nucl. Instr. and Meth. A 482 (2002) 192.
[7] A. Gobbi, A. Mangiarotti, Nucl. Instr. and Meth. A 508 (2003) 23.
[8] W. Riegler, et al., Nucl. Instr. and Meth. A 500 (2003) 144.
[9] W.H. Furry, Phys. Rev. 15 (1937) 569.
[10] W. Feller, An Introduction to Probability Theory and Its Applications, Vol. 1–2, Wiley, New York, 1970, pp. 286, 52.
[11] A. Blanco, et al., IEEE Trans. Nucl. Sci. NS-48 (4) (2001) 1249.
[12] P. Fonte, Nucl. Instr. and Meth. A 456 (2000) 6.
[13] A. Blanco, et al., Nucl. Instr. and Meth. A 508 (2003) 70.
[14] H. Sakai, et al., Nuclear Instr. and Meth. A 484 (2002) 153.